

Selective Interruption of Auditory Interhemispheric Cross Talk Impairs Discrimination Learning of Frequency-Modulated Tone Direction But Not Gap Detection and Discrimination

Katja Saldeitis,^{1,2,3} Marcus Jeschke,^{1,2,3} Annika Michalek,⁴ Julia U. Henschke,⁵ Wolfram Wetzel,¹ Frank W. Ohl,^{1,6,7} and Eike Budinger^{4,7}

¹Department Systems Physiology of Learning, Leibniz Institute for Neurobiology, Magdeburg D-39118, Germany, ²Institute for Auditory Neuroscience, University Medical Center Goettingen, Göttingen D-37075, Germany, ³Cognitive Hearing in Primates Group, Auditory Neuroscience and Optogenetics Laboratory, German Primate Center, Göttingen D-37077, Germany, ⁴Combinatorial NeuroImaging Core Facility, Leibniz Institute for Neurobiology, Magdeburg D-39118, Germany, ⁵Institute of Cognitive Neurology and Dementia Research, Otto von Guericke University, Magdeburg D-39120, Germany, ⁶Institute of Biology, Otto-von-Guericke University Magdeburg, Magdeburg D-39120, Germany, and ⁷Center for Behavioral Brain Sciences, Magdeburg D-39120, Germany

Functional hemispheric lateralization is a basic principle of brain organization. In the auditory domain, the right auditory cortex (AC) determines the pitch direction of continuous auditory stimuli whereas the left AC discriminates gaps in these stimuli. The involved functional interactions between the two sides, mediated by commissural connections, are poorly understood. Here, we selectively disrupted the interhemispheric cross talk from the left to the right primary AC and vice versa using chromophore-targeted laser-induced apoptosis of the respective projection neurons, which make up 6–17% of all AC neurons in Layers III, V, and VI. Following photolysis, male gerbils were trained in a first experimental set to discriminate between rising and falling frequency-modulated (FM) tone sweeps. The acquisition of the task was significantly delayed in lesioned animals of either lesion direction. However, the final discrimination performance and hit rate was lowest for animals with left-side lesioned commissural neurons, demonstrating that also information from the left AC is relevant for FM direction learning. Photolysis after successful learning did not affect the retrieval of the learned task, indicating that the disruption during learning was not because of a general functional impairment. In a second experimental set, the gerbil's ability to detect and discriminate small silent gaps of varying length within FM sweeps was tested. This ability was also preserved after interhemispheric disruption. Taken together, interhemispheric communication between the left and right AC is important for the acquisition of FM tone direction learning but not for its retrieval and for gap detection and gap duration discrimination.

Key words: auditory cortex; chromophore-targeted photolysis; corpus callosum; hemispheric specialization; Mongolian gerbil; rodent

Significance Statement

Hemispheric lateralization of neuronal functions such as speech and music processing in humans are common throughout the brain; however, the involved interhemispheric interactions are ill-defined. Here, we show that the selective photolytic disruption of auditory cortical commissural connections in rodents impairs the acquisition but not retrieval of a frequency-modulated tone direction discrimination task. The final discrimination performance and hit rate was lowest for animals with lesioned left-to-right-side projections; thus, although right auditory cortex is dominant, left auditory cortex is also relevant for learning this task. The detection and discrimination of small gaps within the tone sweeps remain intact, suggesting a pathway for the processing of these temporal structures, which could be independent from the lesioned interhemispheric cross talk.

Received Jan. 29, 2021; revised Jan. 3, 2022; accepted Jan. 5, 2022.

Author contributions: K.S., M.J., W.W., F.W.O., and E.B. designed research; K.S., A.M., and J.U.H. performed research; K.S., A.M., and J.U.H. analyzed data; K.S. wrote the first draft of the paper; K.S., M.J., A.M., J.U.H., W.W., F.W.O., and E.B. edited the paper; K.S. and E.B. wrote the paper.

This work was supported by Deutsche Forschungsgemeinschaft (DFG) Grants SFB TRR31 (to F.W.O. and E.B.) and SFB 779 (to F.W.O.). We thank A. Gürke and J. Stallmann for excellent technical assistance and Dr. Janelle Pakan for helpful comments on an earlier version of the manuscript.

The authors declare no competing financial interests.

Correspondence should be addressed to Eike Budinger at budinger@lin-magdeburg.de.

<https://doi.org/10.1523/JNEUROSCI.0216-21.2022>

Copyright © 2022 the authors

Introduction

The dominance of one cerebral hemisphere in processing certain motor, sensory, and cognitive tasks, is well known in humans and animals (Toga and Thompson, 2003; Hervé et al., 2013; Güntürkün et al., 2020). One of the earliest findings of this functional hemispheric lateralization in humans was the specialization of the left hemisphere for speech and language functions as observed after lesions in Broca's and Wernicke's areas (for historical review, see Hutsler and Galuske, 2003; Harris, 2019).

Subsequent studies demonstrated that the degree of the left-hemispheric dominance can be dependent on individual parameters (Josse and Tzourio-Mazoyer, 2004; Sun and Walsh, 2006; Corballis and Häberling, 2017) but primarily on certain sound features. These include the speed and quantity of temporal and spectral changes, which, in turn, determine the perceived pitch, timbre, prosody, and phrasing of the speech stimuli (Zatorre et al., 2002; Tervaniemi and Hugdahl, 2003; Scott and McGettigan, 2013; Poeppel and Assaneo, 2020). However, while this lateralization linked to properties of speech are well documented in humans, the circuitry underlying this functional dichotomy between hemispheres, as well as the implications for lateralization of general auditory stimuli beyond speech, remain unclear.

In nonhuman primates and other mammals, evolutionary precursors of speech-related and language-related asymmetries most likely exist (for review, see Concha et al., 2012; Güntürkün et al., 2020). Extensive work on Mongolian gerbils trained on auditory discrimination tasks after unilateral or bilateral auditory cortex (AC) lesions demonstrated that certain hemispheric specializations depend on sound continuity or segmentation (Wetzel et al., 1998, 2008; Ohl et al., 1999; Schulze et al., 2014). The results from these and other studies in rats (Rybalko et al., 2006, 2010) and humans (Brechmann and Scheich, 2005; Schönwiesner et al., 2005) revealed that the right AC determines the perceived direction of continuous and segmented frequency-modulated (FM) tones (sweeps) by using global cues, but not the discrimination of gap durations. In contrast, the left AC, by using discrete (local) cues, discriminates gap durations and determines FM directions only when additional segmental information is available. These findings are of particular importance because speech prosody and the macrostructure of musical melodies are predominantly processed in the right hemisphere of humans and are characterized by rather continuous or long spectral and temporal changes (Boemio et al., 2005; Albouy et al., 2020). In contrast, speech phonetics (i.e., the segmentation of speech into phonemes, syllables, words, and sentences) and the microstructure of melodies are predominantly processed in the left hemisphere and are characterized by rather discrete or rapid spectral and temporal changes.

Despite distinct functional lateralization and specializations, both cerebral hemispheres constantly interact via the corpus callosum and the anterior commissure (Bamiou et al., 2007; van der Knaap and van der Ham, 2011). In general, these interhemispheric connections are essential for the functional integration of stimuli from left and right sensory organs, including the perception, recognition, and attention to stimuli (Clarke and Zaidel, 1994; Gazzaniga, 2005; de Haan et al., 2020). Interhemispheric connections are crucially involved in most higher cognitive functions such as visual and verbal memory processing (Blackmon et al., 2015; Paul et al., 2016) and speech comprehension (Bitan et al., 2010; Westerhausen et al., 2009), but our knowledge of their role in auditory learning is limited. In the present study, we therefore investigated the role of interhemispheric cross talk between the left and right primary AC of Mongolian gerbils during auditory discrimination and detection tasks, which encompass lateralized sound processing. To this end, we performed selective photolytic apoptosis of interhemispheric projecting neurons (see Saldeitis et al., 2021), thereby disrupting the information transfer via the corpus callosum and anterior commissure from the left to the right AC and vice versa, before or after learning. We show that this interruption impairs the acquisition

but not retrieval of FM direction discrimination, while the detection and discrimination of gaps in FM tones is preserved. Our results provide important insights into the role of interhemispheric cross talk during auditory learning and into potential compensatory mechanisms after its disturbance.

Materials and Methods

Experimental design

Behavioral experiments were conducted in 77 adult (four- to five-month-old) male Mongolian gerbils (*Meriones unguiculatus*; Charles River) weighing 70–90 g. Three additional gerbils were used for interhemispheric tract tracing only. From the beginning of the experiment, animals were single-housed in a temperature-controlled room (22°C) under a 12-h light (6 A.M. on/6 P.M. off) in standard laboratory cages (Tecniplast, Italy; Eurostandard Type IV, 598 × 380 × 200 mm) with free access to food and water. Surgical procedures and behavioral training have been described in detail previously (Wetzel et al., 2008; Saldeitis et al., 2014, 2021). All experiments were approved by the ethics committee of Sachsen-Anhalt (no. 42502-2-1103 IFN MD), Germany, in accordance with the NIH *Guide for the Care and Use of Laboratory Animals* and the Directive of the European Communities Parliament and Council on the protection of animals used for scientific purposes (2010/63/EU).



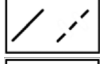
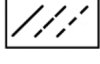
Photolytic lesions of interhemispheric connections

We selectively lesioned the auditory cortical commissural neurons (projecting via the corpus callosum and anterior commissure) using a targeted laser-induced photolytic apoptosis method (Macklis, 1993; Madison and Macklis, 1993; Saldeitis et al., 2021). This method effectively targets retrogradely labeled neuronal populations of interest via the induction of free radicals within the labeled neurons without damaging nearby nonlabeled neurons, glia, or axons of passage (Magavi et al., 2000). We choose the apoptosis method in favor of optogenetic or chemogenetic approaches because it lesions the targeted projection neurons permanently allowing for a longitudinal investigation of the disrupted circuitry in freely behaving animals (Bajo et al., 2010; Homma et al., 2017; Saldeitis et al., 2021).

An 1 mM solution of the photolytic chromophore chlorine e6 (–monoethylenediamineamide) (Phytochlorin, Frontier Scientific) was prepared from 3 ml of 0.01 M phosphate buffer (PB; pH 7.4) and activated with 5 mg N-cyclohexyl-N'-(2-morpholinoethyl)carbodiimide metho-p-toluenesulfonate (Sigma-Aldrich) for 30 min at 4°C on a rocker table (70 rpm). A total of 50 μ l Red Retrobeads™ IX (Lumafuor; excitation: 530 nm, emission: 590 nm) was diluted in 300 μ l PB and added to the solution. Chlorine e6 was then attached to the latex surface of the fluorescent microbeads by gentle agitation on a rocker table at 4°C. The reaction was stopped after 60 min with 335 μ l 0.1 M glycine buffer (pH 8.0). Then, this mixture was pelleted by a series of high-speed centrifugations (Optima MAX Ultracentrifuge, Beckman Coulter, 140,000 × g, 45,000 rpm; MLA-80 rotor, Beckman Coulter) until the supernatant was fully clear. Following each round of 60 min, the supernatant was removed and the pellet was resuspended in 3 ml PB. The final pellet was resuspended in 50 μ l PB and stored at 4°C. Conjugated retrobeads were injected within 14 d. Immediately before use, the vial containing the tracer solution was put into an ultrasound bath (Sonorex Super 10P, Bandelin, 15 min, room temperature) to prevent clotting.

The photolytic tracer was injected into the left or right AC of the animals via stereotaxic pressure injections and under general anesthesia. Anesthesia was induced with a combination of ketamine (10 mg/100 g body weight, i.p.; Ratiopharm GmbH) and xylazine (0.5 mg/100 g body weight, i.p.; Bayer) prepared in isotonic sodium chloride solution. The level of anesthesia was controlled by monitoring the hindlimb withdrawal reflex as well as respiratory rate and maintenance doses were given as needed. Body temperature was maintained at 37°C using a heating blanket. The animals' head was shaved and anesthetized locally with tetracain (Gingicain D, Sanofi) in the region of the incisions (one over the sutura interparietoparietalis and one at a 90° angle, ending at the line connecting the ipsilateral eye and ear canal). Connective tissue and parts

Table 1. Overview of the experimental paradigms and number of animals per group

| Experiment number | Experiment type | Acoustic stimuli | Number of animals | | | |
|-------------------|-------------------------------|---|-----------------------|----------------------|----------|----------|
| | | | Sham _{Beads} | Sham _{NaCl} | Les L->R | Les R->L |
| 1 | FM discrimination acquisition |  | 11* | 10 | 8 | 8 |
| 2 | FM discrimination retrieval |  | 5* | 0° | 6 | 5 |
| 3 | Gap detection |  | 12# | 0° | 9 | 8 |
| 4 | Gap duration discrimination |  | 12# (10/2)+ | 0° | 9 (7/2)+ | 8 (5/3)+ |
| | | | Σ 23 | Σ 10 | Σ 23 | Σ 21 |

* Control animals from experiment 2 were included into 1.

The same animals were used in experiments 3 (training) and 4 (testing).

+ Number of animals tested with the first (long) and the second (short) gap stimulus set, respectively.

° Since experiment 1 revealed that there are no differences in behavioral performance between the two sham-lesioned groups, they were pooled for analysis and in subsequent experiments, only Sham_{Beads} was used. For further information, see Materials and Methods.

of the temporal muscle were carefully detached and deflected. Then, four small holes of 0.5-mm diameter were drilled unilaterally into the skull over the AC (centered over primary field A1) with a dental drill according to stereotaxic coordinates (Radtke-Schuller et al., 2016; bregma: 2.0–3.5 mm caudal, 5.8–6.5 mm lateral, 3.0–4.5 mm ventral) and external landmarks of the bone and vasculature (Budinger et al., 2000). A total of 40 nl of the tracer solution was injected per hole over a period of 2 min via a fine glass micropipette (tip diameter: 20 μm) mounted on an oil hydraulic nanoliter delivery system (WPI). The micropipette was advanced vertically into the brain until the tip, measured from the cortical surface, was 0.8 mm deep. Following the injections, the cranial openings were closed with bone wax (Ethicon), the muscle and skin replaced, and the surgical site was treated with an anti-inflammatory ointment (Volon A, Dermapharm GmbH). The temporal muscle was brought back to its original position and the skin over the cranial opening was closed using surgical silk (Johnson & Johnson) and tissue adhesive (Histoacryl, Braun).

Ten days after the injection, photolytic apoptosis of retrogradely labeled interhemispheric projection neurons was induced by exposure of the contralateral A1 to long-wave laser light under general anesthesia and surgery as described above. The exposed A1 was illuminated transcranially with near-infrared light (670 nm) from a tunable 300 mW laser diode (Flatbeam-Laser 670, Schäfer + Kirchhoff). The laser light was adjusted with beam-shaping optics to create a spot of 1.35-mm diameter focused ~0.8–1 mm deep, and the laser intensity was tuned to 50 mW (surface energy doses of ~1250 J/cm², exposure area ~2.86 mm²) and maintained for 10 min (5 min at two adjacent sites over rostral and caudal A1). The exposure time and intensity was adjusted during prior pilot experiments (not listed here), which had the aim to activate (bleach) the conjugated beads but not to overheat the illuminated brain tissue.

Following illumination, the surgical opening was closed as described above, and the animal was allowed to recover for another 10 d to ensure completed apoptotic processes (Madison and Macklis, 1993; Saldeitis et al., 2021). The unilateral lesions lead to two groups of animals based on the projection direction of the targeted neurons: lesions of neurons projecting from left to right AC (denoted: Les L->R) and lesions of neurons projecting from right to left AC (denoted: Les R->L). Animals receiving tracer injections but no laser treatment (Sham_{Beads}) as well as animals receiving injections of physiological saline (instead of the tracer) plus contralateral laser treatment (Sham_{NaCl}) served as sham-lesioned controls (Table 1).

Training procedures and stimulus characteristics

An overview of the different experimental paradigms is given in Figure 1. Animals were trained and tested in a two-compartment shuttle-box (Hasomed GmbH; 38 × 19 × 22.5 cm, height of the hurdle 4 cm) inside a sound-proof chamber according to one of a set of go/no-go avoidance discrimination paradigms (see FM discrimination and Gap detection/

discrimination further below this paragraph). On the day before the first session (i.e., on the last day of the recovery period), animals were adapted to the shuttle box 20 min without stimuli. Learning experiments were conducted in 10 (FM acquisition, gap detection) plus 5 (FM retrieval, gap discrimination) daily midmorning sessions consisting of 60 trials in FM discrimination experiments or 100 trials in gap detection/discrimination experiments, respectively. Sessions started with an adaptation period of 165 s without presentation of acoustic signals.

Linearly FM tones with rising (FM up) or falling (FM down) modulation directions (FM discrimination task) or FMs up with silent gaps (gap detection/discrimination task) were used as conditioned stimuli (CSs). The continuous FM stimuli consisted of trains of 250-ms-long sweeps (1->2/2->1 kHz frequency, 5-ms rise/decay times, 65–70 dB SPL) separated by 250-ms silent pauses. The gap (segmented) FM stimuli were split by two gaps (ramps: 5 ms) of up to 50-ms duration centered at 50 and 150 ms after sweep onset. Stimuli were delivered free-field by a loudspeaker at the top of the shuttle box. The intertrial intervals were uniformly distributed 18–21 s (FM discrimination task) or 13–19 s (gap detection task) long.

Animals learned to jump from one compartment to the other as response to a CS+ (hit; H) and to stay in same compartment as response to a CS- (correct rejection). Crossing the hurdle within a period of 6 s following a CS- was scored as false alarm (FA) and was punished with a mild electrical foot stimulus (500–700 μA depending the animal's sensitivity threshold, max. 6 s long) applied via the grid floor of the box. This unconditioned stimulus (US) was also applied when the animal failed to jump within 6 s following a CS+ (miss). The occurrence of CS+ and CS- was varied according to a Gellerman pseudorandom schedule.

FM discrimination

Animals had to learn to discriminate the FM tone direction between continuously rising (CS+) versus falling (CS-) FM sweep tones. For the acquisition paradigm (experiment 1; Fig. 1A; Table 1), animals had to learn the task 10 d after they had been lesioned (N_{sham} = 21, including the five control animals from the retrieval experiment 2; N_{Les L->L} = 8; N_{Les L->R} = 8). For the retrieval paradigm (experiment 2; Fig. 1A; Table 1), the training was conducted 10 d after tracer injection, but before laser illumination (N_{sham} = 5; N_{Les R->L} = 5; N_{Les L->R} = 6). Laser treatment was performed after completion of 10 training sessions (CS+: 1–2 kHz continuous FM; CS-: 2–1 kHz continuous FM). The test block consisting of five daily sessions using the same stimuli started 10 d after laser treatment.

Gap detection/discrimination

Lesioned and control animals were initially trained in 10 sessions to discriminate between continuous (i.e., 0-ms gap, CS+) and segmented (50-ms gap, CS-) rising FMs, i.e., they had to detect the gaps in these FMs (experiment 3; Fig. 1B; Table 1; in total: N_{sham} = 12; N_{Les R->L} = 8; N_{Les}

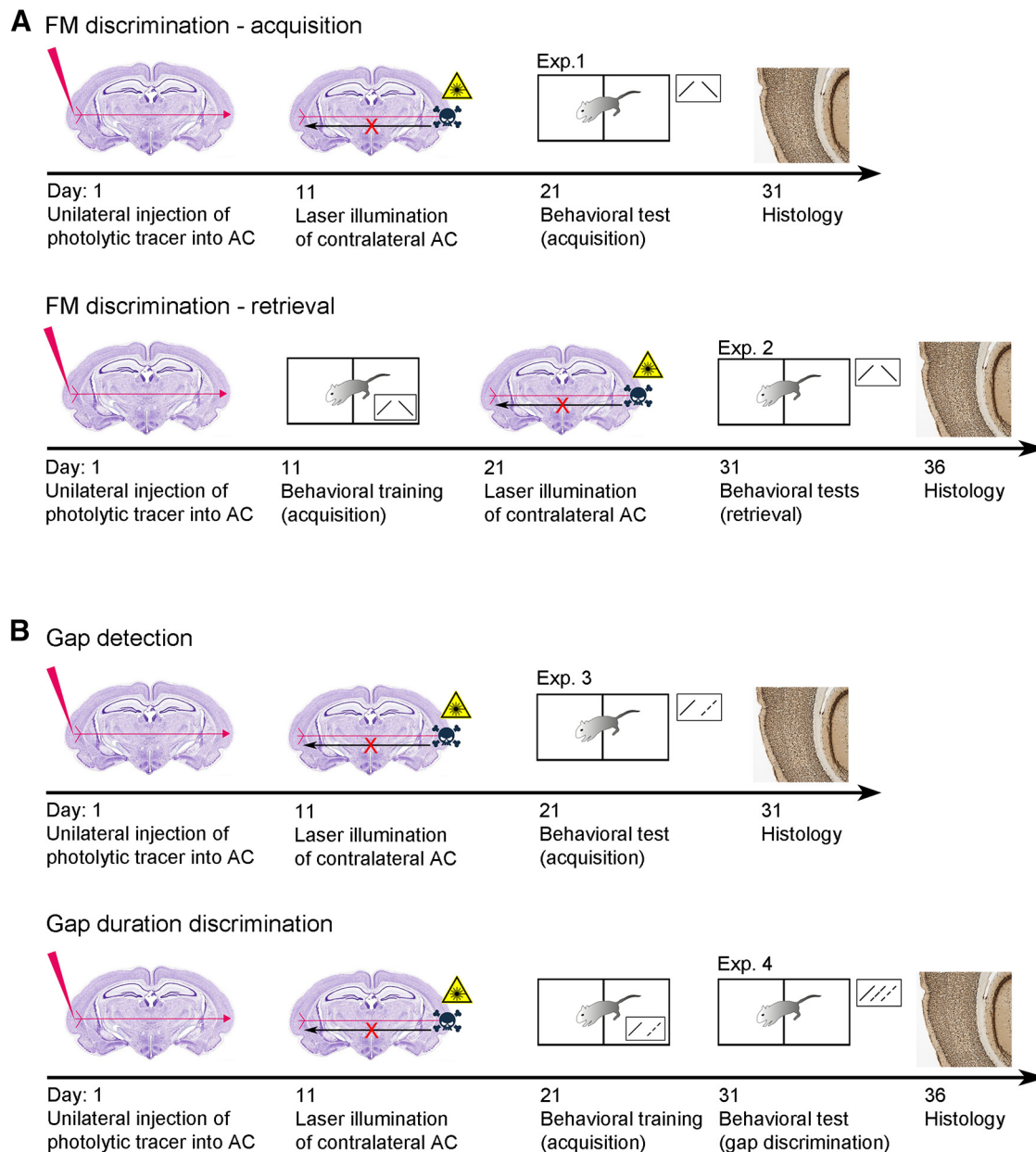


Figure 1. Experimental design and principle of apoptosis method. Sequence of experimental steps according to the different experimental paradigms for the (A) FM discrimination acquisition (Exp. 1) and retrieval (Exp. 2) and the (B) gap detection (Exp. 3) and discrimination (Exp. 4).

$L \rightarrow R = 9$). The animals were then conveyed to five test sessions, in which reinforced continuous and segmented FMs as on training days (given in 2×18 trials) as well as nonreinforced FMs with varying gap lengths were combined in randomized order (experiment 4; Fig. 1B; Table 1). A test session started with a “warm up phase,” consisting of 16 (2×8) trials with CS only, before nonreinforced stimuli were interspersed with the remaining 20 (2×10) CS. The first set of animals ($N_{\text{sham}} = 10$; $N_{\text{Les } R \rightarrow L} = 5$; $N_{\text{Les } L \rightarrow R} = 7$) was tested with gap durations of 10, 15, 17, 19, 21, 23, 25, and 30 ms, consistent with a prior study on gerbils (Wetzel et al., 2008). However, since our results suggested that in the current study shorter gaps were more suited to detect the dependency of responses on gap duration, an additional set of animals ($N_{\text{sham}} = 2$; $N_{\text{Les } R \rightarrow L} = 3$; $N_{\text{Les } L \rightarrow R} = 2$) was tested using nonreinforced stimuli with 0 (ramps only)-, 1-, 2-, 4-, 7-, 10-, 15-, and 21-ms gaps.

Statistical analysis of behavioral experiments

As measures of discrimination performance in acquisition and retrieval experiments (experiments 1–3) the difference between H (CR+) rate and FA (CR-) rate was used (CR rate difference; Figs. 3A, 4A, 5A, top)

as well as values of the parametric detectability index d' [($d' = z(H) - z(FA)$), where $z(H)$ and $z(FA)$ are the z transforms of H rate and FA, respectively; Figs. 3A, 4A, 5A, middle]. Further, in acquisition conditions, the learning performance was assessed by how quickly animals learned the task (first of at least two consecutive sessions with significant performance, Fisher's test, $p < 0.01$, which we termed learning speed; Schulze et al., 2014) and the final discrimination performance (median of the differences between CR+ and CR- rates across the last four training sessions; Schulze et al., 2014). Between-group comparisons for learning speed and final discrimination performance were conducted using Kruskal–Wallis tests and for all *post hoc* pairwise comparisons Holm–Bonferroni-corrected Mann–Whitney U statistics. Additionally, Kolmogorov–Smirnov tests were employed to compare the distributions of learning speeds between pairs of animal groups. In the retrieval condition, possible effects of interhemispheric lesioning were determined from the individual median differences of CR rates of 5 test sessions using the Kruskal–Wallis test.

In the gap discrimination task (experiment 4; Fig. 5), response rates were averaged from 5 test sessions (because of the small number of

repetitions per nonreinforced stimulus and trial). For this, the 16 first “warm-up” trials were not considered, since animals tended to respond less frequently to CS+ during the intersperse-phase (in which CS+ occurred less often). To identify potential differences in gap detection between groups, psychometric curves of individual animals were fitted with a Weibull function. The detection thresholds were defined as the gap durations halfway between the maximum and minimum response rate and compared by means of the Kruskal–Wallis test. In addition, normalized response rates to the 10-ms gap segmented FMs, which was the shortest gap stimulus common to both stimulus sets, were compared (Table 2). Furthermore, we performed a binomial logistic regression using MATLAB’s fitglm function, with behavior (jump, stay) on each trial as the response variable, gap duration and experimental group (Sham, Les L->R, Les R->L) as fixed effects, and subject as random effect [Response ~ Group*GapLength_{adj} + (1|Animal); generalized linear mixed-effect model (GLMM); Fig. 5D]. To allow distinction between the continuous FM stimulus CS+ and the 0-ms gap stimulus (ramps only), the ramp duration (5 ms) was added to each gap stimulus length (GapLength_{adj}).

Graphing and statistical analyses were performed with MATLAB (The MathWorks Inc).

Immunohistochemistry and histologic analysis

On the day after the last behavioral experiment (Fig. 1), animals were reanaesthetized and perfused transcardially with 20 ml of 0.1 M PBS (pH 7.4) followed by 4% paraformaldehyde in PBS (PFA; 200 ml). Brains were postfixed in 4% PFA overnight, cryoprotected in 30% sucrose, frozen at -50°C in isopentane, and cut on a cryostat (Leica CM 1950) into 50- μm -thick horizontal sections. Every first and second section was directly mounted on slides and coverslipped using Immu-Mount (Thermo Fisher Scientific) to analyze the injection site and retrograde transport of beads (Fig. 2A). To assess the efficacy of the laser treatment, indicated by a reduction of cell numbers in Layers III and V, every third section was stained for neuronal nuclei using a mouse anti-NeuN antibody (1:500, overnight, Chemicon/Millipore Europe, catalog #MAB 377, RRID: AB_2298772; solution containing 0.1–0.3% Triton X-100, 1% bovine serum albumin). The NeuN antibody was visualized by means of a biotinylated goat anti-mouse secondary antibody (1:200, 2 h, Vector Labs, catalog #BA-9200, RRID: AB_2336171) and the avidin-biotin-peroxidase method (Vectastain Elite ABC kit, Vector Labs) and using 3,3'-diaminobenzidine (Sigma-Aldrich) as chromogen. Then, the sections were mounted on gelatin-coated slides, dehydrated, and coverslipped with Merckoglass (Merck).

To determine the layer-specific ratio of interhemispheric projection neurons on all neurons in A1, brains of three additional animals, which were injected with conjugated Red Retrobeads but not laser-treated, were processed as described above; however, the NeuN antibody was visualized by a green fluorescent secondary antibody (anti-mouse Alexa Fluor 488; 1:200, 2 h, Invitrogen by Thermo Fisher Scientific, catalog #A11017, RRID: AB_143160). Commissural neurons appeared double-labeled (Fig. 2C).

Microscopic analyses and photography were conducted using a combined light and epifluorescence microscope (Zeiss Axioskop 2) fitted with the appropriate filter sets and a digital camera (Leica DFC 500) except for the double-staining experiments. Here, sections were scanned in five to seven confocal planes at 5 \times magnification using a confocal microscope (Zeiss LSM 700).

Quantitative validation of targeted photolysis was performed in 18 example animals (13 lesioned and 5 controls) using ImageJ (<http://imagej.nih.gov/ij/>). Lesioned animals were from the acquisition (three Les L->R, three Les R->L), retrieval (three Les L->R, 1 Les R->L), and gap detection/discrimination groups (2 Les L->R, 1 Les R->L). Since we did not expect any toxicity effects of the NaCl injections or laser illumination alone (based on pilot experiments), control animals were all from the Sham_{Beads} group (two left and three right injected, all FM acquisition). The image analysis was performed largely blind to the experimental group and injected hemisphere (though observer could see the injection site in some images). To calculate a proxy of neuronal cell loss in Layers III and V of the lesioned relative to the nonlesioned side, RGB

images of NeuN-stained sections were converted first nonweighted into 16-bit images (gray scale), and then into binary images by choosing a reasonable threshold resulting in separated neuronal somata (Fig. 2B). The same threshold was applied for all sections of a given animal and it was similar across animals. Then, the ImageJ standard watershed algorithm was applied for particle separation. Finally, individual cortical layers were outlined in both the lesioned (laser-illuminated side) and the nonlesioned (tracer-injected side) A1 and the relative area occupied by (black) particles (i.e., NeuN-positive neurons) versus (white) neuropil was determined in at least three sections per hemisphere as a measure of neuronal density.

The overall ratio of commissural neurons on all A1 neurons was determined by counting single-stained NeuN-positive neurons and double-labeled tracer containing neurons in the different cortical layers using the Cell Counter plugin of ImageJ (Fig. 2C). Basically, for each of the three brains used, five sections of 150- μm distance, covering the homotopic region within A1 contralateral to the injection sites, were selected. Then, the six cortical layers were delineated on the basis of their cytoarchitectonic features (Budinger et al., 2000) as regions of interest and differentially labeled cells were counted manually.

Results

Photolytic apoptosis lesions interhemispheric projection neurons

First, we investigated whether our laser-induced photolytic apoptosis approach selectively lesions auditory commissural neurons and consequently disrupts their interhemispheric projections. Therefore, we compared the relative number of neurons at the intact ipsilateral tracer injection site with the contralateral side of retrogradely labeled and subsequently lesioned commissural neurons.

Figure 2A depicts a typical example of an injection site of conjugated retrobeads centered in Layer V of the ipsilateral A1 and of the laminar location of retrogradely labeled neuronal somata in the contralateral A1. The resulting pattern of labeling shows that A1 receives contralateral cortical input mainly from Layer V, but also from other layers, in particular Layer III (see also Fig. 2C). Targeted apoptosis of the interhemispheric projection neurons resulted in a reduction of NeuN staining density, i.e., the number of most likely commissural neurons, in these cortical layers of the hemisphere contralateral to injection (Fig. 2B). Quantitative analysis revealed a reduction of $13.8 \pm 3.1\%$ (mean \pm 1 SEM) of the area covered by neuronal nuclei in Layer V and $3.0 \pm 2.3\%$ of the area covered by neuronal nuclei in Layer III of AC (Fig. 2C). Within the analyzed control group (Sham_{Beads}) there was no noticeable reduction of the neuronal density ($3.1 \pm 2.1\%$ in Layer V, $-2.2 \pm 1.8\%$ in Layer III).

To determine the efficiency of interhemispheric lesions one has to know the percentage of commissural neurons in the cortical layers of the AC. Since, to the best of our knowledge, no such data are available in the literature, we performed additional double-labeling tracing experiments in 3 animals (Fig. 2C). The ratio of single-labeled NeuN-stained neurons versus double-labeled (tracer + NeuN) showed that $16.7 \pm 1.3\%$ (mean \pm 1 SEM) of neurons in Layer V and $6.3\% \pm 1.0\%$ of neurons in Layer III provide commissural connections to the contralateral A1. This suggests that our lesions included, on average, close to all commissural neurons in Layer V and approximately half of the commissural neurons in Layer III.

Discrimination learning of FM tone direction is impaired by disrupted interhemispheric cross talk

We next sought for functional consequences of disrupted interhemispheric connections in auditory discrimination learning of

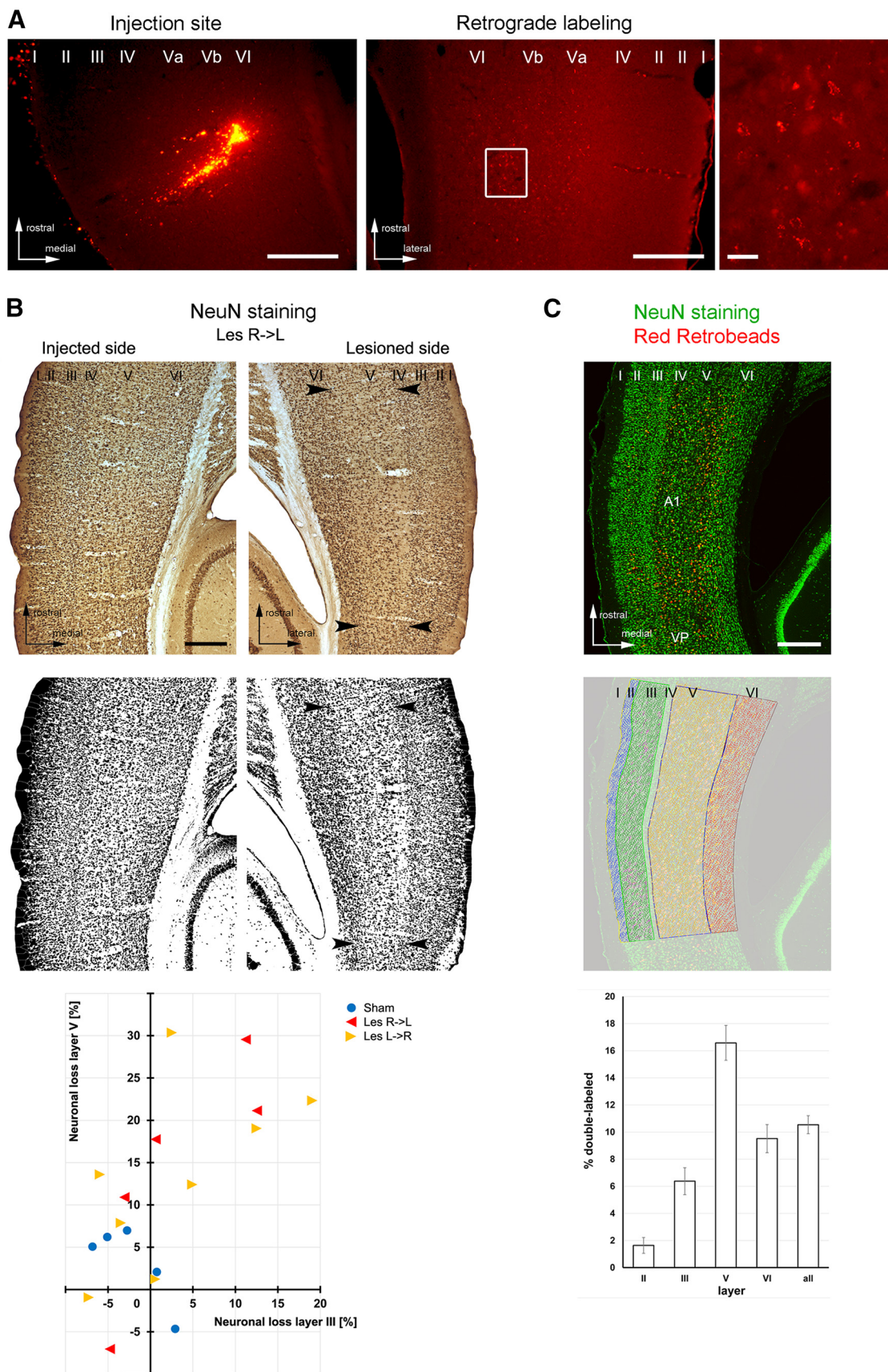


Figure 2. Histologic analysis of the retrograde transport between auditory cortices of both hemispheres, the degree of photolytic lesions, and overall ratio of auditory commissural neurons. **A**, Retrograde labeling of interhemispheric neurons. Left panel, Photograph showing an injection site of red fluorescent (diorine-e6-conjugated) beads into left A1 from the Sham^{Beads} group. Scale bar: 400 μ m. Middle panel, Corresponding retrograde labeling in all layers of the contralateral A1. Scale bar: 400 μ m. Right panel, Enlarged view of labeled neurons in Layer V (white box of middle panel; scale bar: 20 μ m). **B**, Top and middle, Original and binary converted images of NeuN-stained horizontal brain sections showing neuronal apoptosis in Layer V of the lesioned illuminated cortical

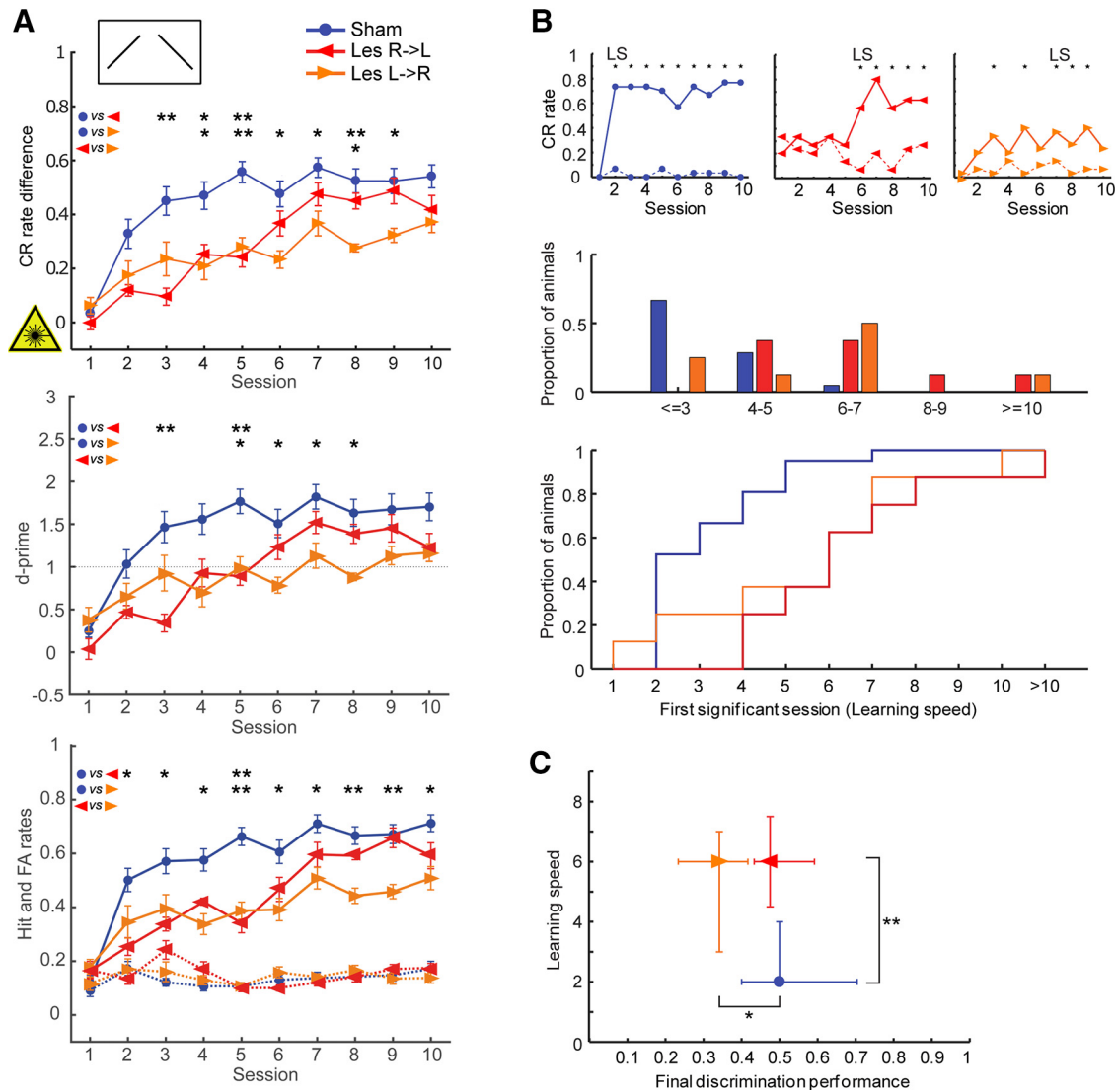


Figure 3. Effects of interhemispheric lesions on the ability to discriminate between falling and rising continuous FM tones (250-ms duration, CS+: 1–2 kHz, CS–: 2–1 kHz), when the lesion was induced before training (acquisition paradigm, experiment 1). **A**, top, Learning curves show the mean (± 1 SEM) of behavioral performance (CR rate difference: H rates minus FA rates) of lesioned and control animals in daily sessions. Lesioned animals took more sessions to acquire the direction discrimination task (see also **B**, **C**). Note that the Les L->R animals learned the task not as well as the other animals (see also **C**). Middle, Mean ± 1 SEM values of the parametric detectability index d-prime [($d' = z(H) - z(FA)$), where $z(H)$ and $z(FA)$ are the z transforms of H rate and FA, respectively]. Controls perform better than Les R->L animals during sessions 3 and 5, and better than Les L->R in sessions 5–8, comparable to CR differences measures. d-prime = 1 is indicated, which corresponds to a signal strength of 1 SD above noise. Bottom, Mean \pm SEM of H (solid lines) and FA (dashed lines) rates. Performance differences between groups mainly based on differences in H rates. $N_{\text{sham}} = 21$; $N_{\text{Les R->L}} = 8$; $N_{\text{Les L->R}} = 8$. Between-group comparisons for each session were conducted using Holm–Bonferroni-corrected Mann–Whitney U statistics; * $p < 0.05$, ** $p < 0.01$. **B**, top, Representative individual example learning curves showing Hs (solid line) and FAs (dotted line). Sessions with significant discrimination (*) as well as the learning speed (LS; first of at least two consecutive sessions with *) are indicated. Middle, Histograms showing the distribution of learning speed (LS) for each group. Sessions were binned into five time periods. Bottom, Step graphs depicting the cumulative learning speed. Between-group comparisons of learning speed distributions were conducted using Holm–Bonferroni-corrected Kolmogorov–Smirnov tests. Sham versus Les R->L: $p = 0.0167$, Sham versus Les L->R: $p = 0.0485$, Les R->L versus Les L->R: $p = 0.9290$. **C**, Scatter plot of learning speed versus final discrimination performance (DP; median of the CR rate differences across the last 4 training sessions). Given are median values and quartiles. Between-group comparisons were conducted using Holm–Bonferroni-corrected Mann–Whitney U statistics; * $p < 0.05$, ** $p < 0.01$.

side of A1 (e.g., between arrowheads), discernible by its reduced cell density compared with the nonlesioned injected side. Scale bar: 400 μm . Bottom, Quantitative analysis of neuronal cell loss in Layers III and V of the lesioned compared with the nonlesioned side in 18 example animals (for individual numbers, see Materials and Methods). **C**, top, Confocal image (maximum intensity projection) of AC showing all NeuN+ cells (i.e., all neurons; green) and tracer-labeled cells (red/yellow) after injections of Red Retrobeads into the contralateral A1. Scale bar: 400 μm . Middle, Same image with the overlay of manually counted neurons and tracer-labeled neurons in the different AC layers using the Cell Counter plugin of ImageJ. Bottom, Percentage of neurons (mean ± 1 SEM) projecting to the contralateral A1 across different AC layers ($n = 3$). Layers I and IV did not contain retrogradely labeled neurons. I–VI, cortical layers I–VI; A1, primary auditory field; VP, ventroposterior auditory field.

FM direction, which has been previously demonstrated to be dominated by right-hemispheric AC processing. First, we tested the role of interhemispheric communication on the acquisition of this task (experiment 1; Fig. 1A; Table 1). Animals had to learn the discrimination between a rising (CS+) and a falling (CS–) continuous FM sweep. In general, lesions of auditory cortical interhemispheric connections induced before training delayed the acquisition of the learning task compared with control animals (Fig. 3A). Thereby, Les R->L animals had significantly worse performance in terms of CR rate difference on sessions 3–5 and Les L->R animals on sessions 4–

9. On day 8, the performance of the Les L->R was significantly lower than of the Les R->L animals. Performance differences between groups were mainly based on differences in H rates; the FA rates were relatively constant over all sessions for all three experimental groups. Thereby, Les L->R but not Les R->L animals had significantly lower Hs in sessions 6–10 than the controls, indicating that particularly the FM task acquisition of the Les L->R animals was disturbed.

To further compare learning performances, we determined the learning speed (defined as the first session of at least two consecutive sessions with a significant difference between CS+ and CS- induced hurdle crossings, Fisher's test, $p < 0.01$; Fig. 3B, C) and final discrimination performances (defined as the median of the differences between H (CR+) and FA (CR-) rates across the last four training sessions of each individual animal; Fig. 3C). The learning speed distributions of control and lesioned animals were significantly different (Holm–Bonferroni-corrected Kolmogorov–Smirnov tests: Sham vs Les R->L, $p = 0.0167$; Sham vs Les L->R, $p = 0.0485$; Les R->L vs Les L->R, $p = 0.9290$). The relative frequency and cumulative distributions of learning speed for each group revealed that lesioned animals achieve significant performance later than control animals (Fig. 3B). While >50% of the control animals were able to discriminate the FMs during session 2 and ~95% by session 5, lesioned animals showed a more gradual increase of the cumulative learning speed distribution. The median learning speed was fastest in control animals (two sessions), while Les L->R and Les R->L animals had a median of six sessions (Fig. 3C; $p = 0.0024$, Kruskal–Wallis ANOVA). Pairwise comparisons show significant differences only for Sham versus Les R->L (Holm–Bonferroni-corrected Mann–Whitney U test; $p = 0.002$) because of the larger variance of learning speed in the Les L->R group (Fig. 3B, middle). The final discrimination performance of control and Les R->L animals converged on similar levels, while Les L->R animals were not able to fully catch up their lag within 10 sessions (Fig. 3C; $p = 0.0233$).

There was no correlation between the behavioral performance of the animals in terms of final performance and learning speed with the degree of the lesion in cortical Layers V and III ($n = 11$; 6 lesioned and 5 control animals; Pearson correlation; Table 3).

We then investigated effects of disrupted auditory interhemispheric connections on the retrieval of the learned FM direction discrimination (experiment 2; Figs. 1A, 4; Table 1). In contrast to the acquisition task, no impairment in the retrieval of the discrimination performance was observed when laser illumination was conducted after successful training (Fig. 4B; Kruskal–Wallis test; $p = 0.9433$). The slight drop of performance for all animals between the last training before (session 10) and the first test session after (11) the lesion, which was because of a slight decrease in the H and increase in the FA rates (Fig. 4A, bottom), was not significant in any of the groups (Wilcoxon signed-rank test).

In summary, photolytic apoptosis of interhemispheric neurons before training impairs the animals' ability to learn to discriminate between a rising and a falling continuous FM sweep; however, photolysis of commissural neurons after successful learning did not affect the retrieval of the learned task. This also suggests that there is no specific functional deficit in processing FM sweeps after interhemispheric lesions, but that the commissural connections between primary auditory regions specifically function as a learning capacity in this regard. Since H and FA rates of lesioned and control animals show generally similar

trends there seem to be no different strategies in the acquisition and retrieval of the task in all animals. The direction of the lesion mainly affected the discrimination performance toward the end of the training sessions with the final discrimination performance and H rate being lower for Les L->R than for Les R->L animals. This indicates that despite the dominance of the right AC in discrimination learning of FM tone direction the left AC contributes to solving this task.

Gap detection and discrimination are not affected by disrupted interhemispheric cross talk

Next, we investigated the influence of interhemispheric cross talk on auditory gap discrimination learning, a task, which has been demonstrated to be lateralized toward the left AC.

Initially, animals were trained to discriminate between a rising continuous FM (CS+) and a rising segmented FM sweep (CS-), i.e., they had to detect a 50-ms gap in these stimuli (experiment 3; Fig. 1B; Table 1). There was no difference in the performance between control and lesioned animals as seen in the learning curves, H and FA rates (Fig. 5A), learning speed (Kruskal–Wallis, $p = 0.1591$; Kolmogorov–Smirnov, $p > 0.05$ for all pairwise comparisons; not shown), and final discrimination performance (Kruskal–Wallis, $p = 0.4514$; not shown). This indicates, that the general ability for detecting larger gaps in FMs is still preserved following disruption of auditory cortical interhemispheric communication.

In further test sessions (experiment 4; Fig. 1B; Table 1), we investigated possible effects of interhemispheric lesions on responses to segmented FMs with varying shorter gap durations. For this purpose, we interspersed both the CS+ (continuous FM) and CS- (50-ms segmented FM) with untrained nonreinforced gap stimuli having 10-, 15-, 17-, 19-, 21-, 23-, 25-, and 30-ms gap durations. The intention was to identify a discrimination threshold in case the animals behaviorally assign shorter-gap stimuli to the CS+ and longer-gap stimuli to the CS-. However, there was no significant difference in response rates between lesioned and nonlesioned animals (except for 23 ms because of a very short response rate in the control animals; Fig. 5B, upper panel/cohort 1; Mann–Whitney U test with Holm–Bonferroni-correction, $p > 0.05$) and no (linear or monotonic) relationship between response rates and gap durations. Together, this demonstrates that also the discrimination between continuous FMs and FMs with gaps of 10–30 ms is not affected by a disturbed interhemispheric cross talk.

Since there was no apparent relationship between response rate and gap duration (i.e., animals detected shorter and longer gaps equally easy) but a steep increase in response rates from the shortest gap duration (10 ms) to the CS+, we tested additional animals with gaps of 0 (ramps only)-, 1-, 2-, 4-, 7-, 10-, 15-, and 21-ms duration (Fig. 5B, lower panel/cohort 2). Using this stimulus set, a relationship between gap duration and response rate was observed in all seven animals (Pearson's correlation coefficient; $p < 0.05$ for each animal; for group means see Table 2). Then, we sought to identify possible differences in gap detection threshold between lesioned and control groups. Therefore, psychometric curves of individual animals were fitted with a Weibull function (Fig. 5C). 50% thresholds determined from the data collected using the second stimulus set (i.e., shorter gaps) lay within the same range as those determined from the long gap dataset (Table 2); hence, we joined them for statistical analysis. The mean thresholds were around 10 ms (Sham: 8.20 ms, Les R->L: 9.23 ms, Les L->R: 11.47 ms). The data do not suggest differences between groups with respect to their 50% thresholds

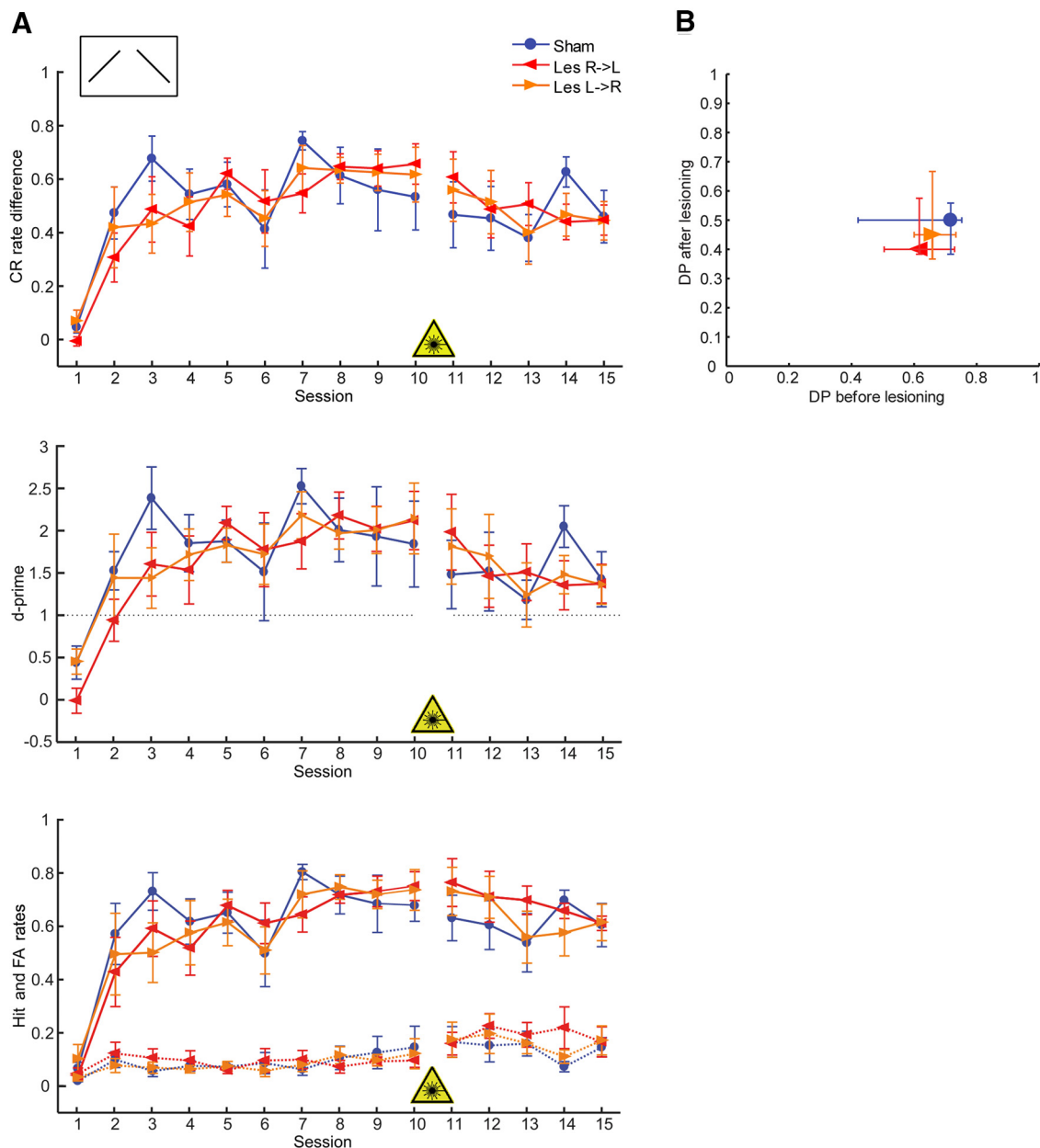


Figure 4. Effects of interhemispheric lesions on the ability to discriminate between falling and rising continuous FM tones (CS+: 1–2 kHz, CS–: 2–1 kHz), when the lesion was induced after training (retrieval paradigm, experiment 2). **A**, top, Learning curves show the mean (± 1 SEM) of behavioral performance (CR rate difference) of lesioned and control animals in daily sessions. Middle, Mean ± 1 SEM values of the parametric detectability index *d*-prime. Bottom, Mean ± 1 SEM H (solid lines) and FA (dashed lines) rates. There are no significant differences between experimental groups; thus, lesioning interhemispheric connections after successful acquisition did not change task performance. $N_{\text{sham}} = 5$; $N_{\text{Les R->L}} = 5$; $N_{\text{Les L->R}} = 6$. For other conventions see Figure 3A. **B**, Scatter plot of retrieval discrimination performance (median of the 5 test sessions) versus discrimination performance during the last four training days before laser illumination (final DP; see Fig. 3C). Given are median values and quartiles. Mann–Whitney *U* statistics did not reveal any significant between-group differences.

(Kruskal–Wallis, $p = 0.1390$) and to higher thresholds, albeit control animals tended to have smaller thresholds. Also, the shortest common gap duration (10 ms) was detected with similar frequency in all groups (Kruskal–Wallis, $p = 0.1867$; Table 2). Finally, we performed a GLMM analysis with behavior (jump, stay) on each trial as the response variable, gap duration and experimental group as fixed effects, and subject as random effect (Fig. 5D). This analysis did not reveal significant differences between experimental groups (ANOVA; $p = 0.314$) as well.

Taken together, the interruption of interhemispheric cross talk between the auditory cortices does not impair the detection and discrimination learning of larger (50 ms) as well as smaller gaps in FMs. In comparison to our previous studies on gerbils

(Wetzel et al., 2008), the detection threshold is smaller than expected, namely, around 10 ms.

Discussion

The present study demonstrates specific consequences of unidirectional lesions of auditory cortical interhemispheric connections on FM tone direction discrimination and gap detection learning. Photolytic apoptosis of interhemispheric neurons before training impairs the animals' learning ability to acquire the discrimination between a rising and a falling continuous FM tone sweep. That is, lesioned animals need longer than controls to learn the task; however, eventually all animals learn to solve it

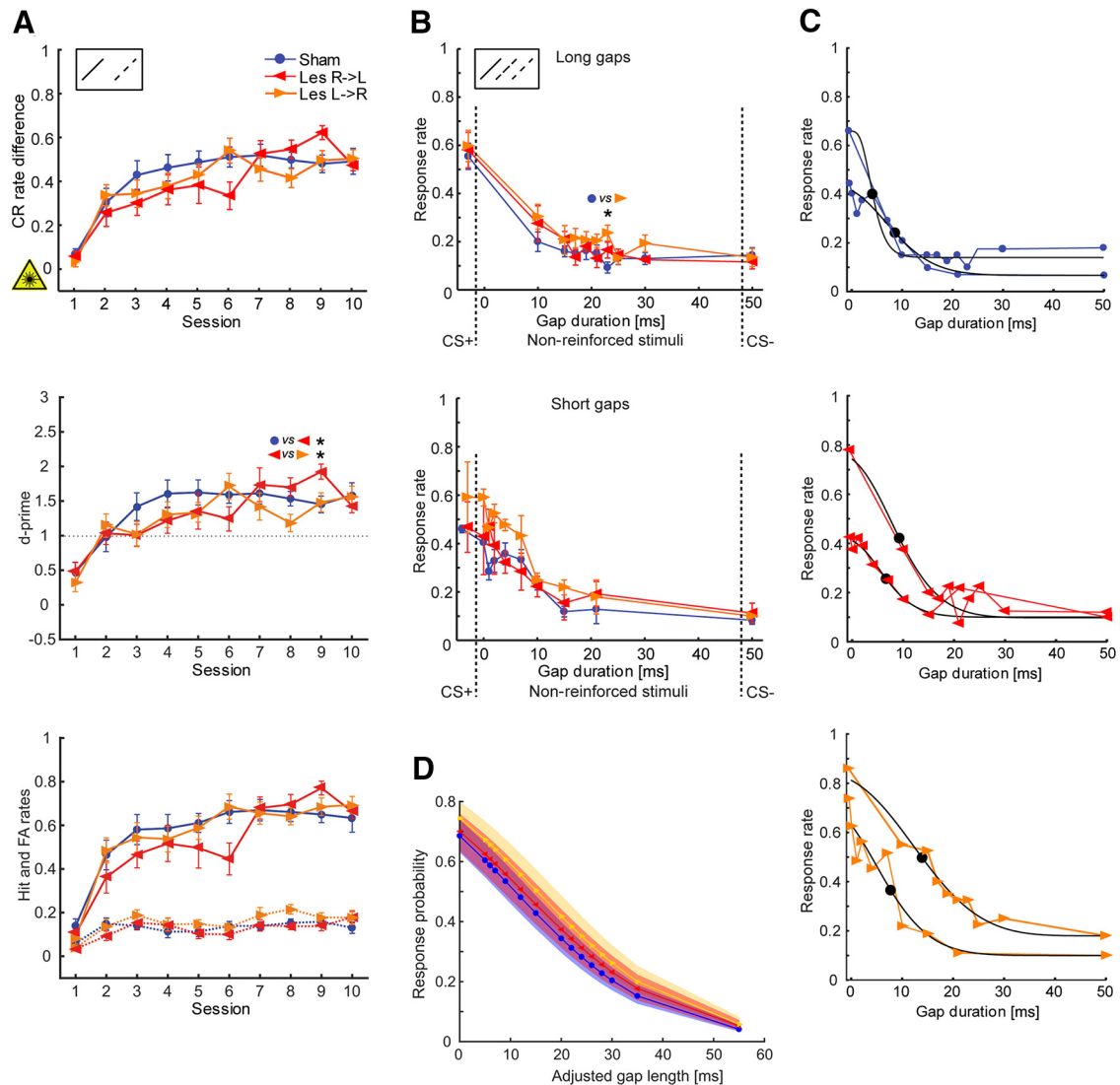


Figure 5. Effects of interhemispheric lesions on the ability to detect and discriminate between gaps in FM tones. Lesions were induced before training. **A**, Learning curves (CR rate difference; top), parametric detectability index (d' ; middle) as well as H and FA rates (bottom) of lesioned animals that were trained to discriminate rising continuous (CS+: 1–2 kHz, no gaps) versus rising segmented (CS–: 1–2 kHz, two 50-ms gaps) FM sweeps (experiment 3). There are no significant group differences between performances (except for d' in session 9); thus, interhemispheric lesioning did not affect the task performance in general. $N_{\text{sham}} = 12$; $N_{\text{Les R->L}} = 8$; $N_{\text{Les L->R}} = 9$. Between-group comparisons for each session were conducted using Holm–Bonferroni-corrected Mann–Whitney U statistics; $*p < 0.05$. For other conventions see Figure 3A. **B**, Responses to reinforced and nonreinforced FM stimuli segmented by varying gap durations (experiment 4). CS+ with no gaps and CS– with 50-ms gaps (as in experiment 3) were used as reinforced stimuli. Top, Response rates of animals tested with gap stimuli of 10-, 15-, 17-, 19-, 21-, 23-, 25-, and 30-ms gap durations (cohort 1, long gaps). Given are means \pm SEM. $N_{\text{sham}} = 10$; $N_{\text{Les R->L}} = 5$; $N_{\text{Les L->R}} = 7$. Bottom, Response rates of animals tested with gap stimuli of 0 (ramps only)-, 1-, 2-, 4-, 7-, 10-, 15-, and 21-ms gap durations (cohort 2, short gaps). $N_{\text{sham}} = 2$; $N_{\text{Les R->L}} = 3$; $N_{\text{Les L->R}} = 2$. Response rates were determined from five test sessions. Between-group comparisons for each stimulus were conducted using Holm–Bonferroni-corrected Mann–Whitney U statistics; $*p = 0.0151$. **C**, Psychometric curves of individual animals (one animal per lesion group and stimulus cohort) fitted with a sigmoid Weibull function (black curves). The fitting served to identify possible differences in gap detection threshold (50%, indicated by a dot in the black curve). For average gap lengths at 50% performance threshold of all groups see Table 2. There are no differences between control and lesioned animals. **D**, GLMM analysis of behavioral data for gap detection and discrimination. Fitted response probabilities (95% confidence intervals) to different gap lengths (GapLength_{adj}; see Materials and Methods) using trial based binomial logistic regression. There is no difference between groups (ANOVA, $p = 0.314$). Response probability is higher for shorter gap lengths since animals were trained to change the compartment in response to a continuous FM and to stay in the compartment when a gap was detected.

suggesting that only learning-specific and not general functional mechanisms are impaired. When the projections from the left to the right AC are disrupted, the final discrimination performance and H rate is lower than in control animals and animals with a disruption the other way round suggesting a specific, most likely supportive rather than dominant role of the left AC in FM direction discrimination. Photolysis after successful learning does not affect the retrieval of the task again indicating a specific role of interhemispheric commissural connections in acquisition learning of this task. Likewise, the discrimination learning of a rising continuous

FM versus a rising segmented FM sweep was also preserved after interhemispheric cross talk disturbance and gap detection thresholds were similar across the intact and lesioned experimental groups.

Functional anatomy of interhemispheric cross talk

It is still an open question whether commissural connections functionally have a rather excitatory or inhibitory influence onto the contralateral hemisphere, which may be influential for sharing and integrating information or maintaining independent

Table 2. Comparison of performances in the gap detection task

| | | Sham | Les R-> L | Les L-> R |
|---|---------------|--------------------|--------------------|---------------------|
| Linear correlation coefficients (performance vs gap length) | Long gap set | -0.28 ± 0.44 | -0.42 ± 0.47 | -0.39 ± 0.39 |
| | Short gap set | -0.83 | -0.811 ± 0.07 | -0.91 |
| Response rate at 10-ms gap stimulus (normalized) | Total | 0.31 ± 0.24 | 0.37 ± 0.18 | 0.38 ± 0.12 |
| | Long gap set | 0.29 | 0.42 | 0.41 |
| | Short gap set | 0.39 | 0.29 | 0.29 |
| Gap length at 50% performance threshold (fitted) | Total | 8.20 ± 2.98 ms | 9.23 ± 4.54 ms | 11.47 ± 3.28 ms |
| | Long gap set | 7.84 ms | 10.23 ms | 11.76 ms |
| | Short gap set | 10.02 ms | 7.47 ms | 10.49 ms |

Linear correlation between response rate and gap length. Response rates to 10-ms gap stimulus (rate normalized between minimum and maximum response) as well as 50% thresholds for each experimental group are given (means \pm 1 SD; long gap set = experiment 3; short gap set = experiment 4).

For further information, see Results.

Table 3. Linear correlation between behavioral performance and degree of lesions in Layers V and III in the FM acquisition task

| | Correlation values | |
|---|--------------------|----------|
| | <i>r</i> | <i>p</i> |
| Final DP vs lesion degree Layer V | -0.2553 | 0.4486 |
| Final DP vs lesion degree Layer III | 0.0451 | 0.8953 |
| Learning speed vs lesion degree Layer V | 0.4965 | 0.1203 |
| Learning speed vs lesion degree Layer III | 0.2460 | 0.4659 |

Person correlation, $n = 11$.

processing across hemispheres (for review, see Bloom and Hynd, 2005; van der Knaap and van der Ham, 2011). In the AC, experimental evidence has been obtained for both types of effects using, for example, electrical, pharmacological, cooling, and optogenetic techniques (Kitzes and Doherty, 1994; Richter et al., 1999; Carrasco et al., 2013; Slater and Isaacson, 2020). The interhemispheric cross talk is mediated by a complex neuroanatomical substrate, which involves both excitatory and inhibitory commissural neurons, which, in turn, terminate on both excitatory pyramidal neurons and inhibitory interneurons (for AC, Cipolloni and Peters, 1983; Code and Winer, 1985; Rock et al., 2018; for review, see Conti and Manzoni, 1994; Karayannis et al., 2007). Thus, behavioral effects of lesioning interhemispheric connections can be expected to be diverse. In gerbils (Budinger et al., 2000; Thomas and López, 2003) and other mammals (e.g., cats: Lee and Winer, 2008; mice: Rock and Apicella, 2015), auditory interhemispheric cortical neurons are predominantly located in Layers V and III (for review, see Budinger, 2020). In our current study, the neuronal degeneration as investigated by a relative density analysis with the neuronal marker NeuN was strongest in Layer V; thus, the majority of behavioral effects can be attributed to Layer V based interhemispheric disruptions. Information about the ratio of interhemispheric projection neurons on the total of all neurons across AC layers is, to the best of our knowledge, not available from the literature. Thus, we performed additional experiments to determine this ratio. We found that \sim 16.6% of the neurons in Layer V and 6.4% in Layer III provide commissural connections to the homotopic area of the contralateral AI. Consequently, on average, nearly all of the Layer V and approximately half of the Layer III connections were lesioned in our behavioral experiments.

Disruption of interhemispheric cross talk impairs the acquisition of FM direction discrimination

We show that an interrupted interhemispheric transfer delays discrimination learning of FM tone direction in Mongolian gerbils. Previous studies employing similar stimuli have demonstrated the essential and dominant role of the right AC in performing this task (e.g., gerbil: Wetzel

et al., 1998, 2008; rat: Rybalko et al., 2006; human: Poeppel et al., 2004; Brechmann and Scheich, 2005; König et al., 2008). Our results support this notion and provide evidence that only an intact interhemispheric cross talk enables its proper acquisition, i.e., lesioned animals in either direction take significantly longer to acquire the task. However, these animals are still able to learn the discrimination with sufficient training. This suggests that the disrupted function of the interhemispheric auditory cortical connections can be compensated by other mechanisms (Paiement et al., 2010; Bartolomeo and Thiebaut de Schotten, 2016; Roland et al., 2017). These compensation mechanisms seem to be rather rapid (within a few days) and may include alternative crossing subcortical pathways (e.g., commissure of the inferior colliculi: Pollak et al., 2003) but most likely cortical routes, for example, via commissural connections of higher cortical areas (e.g., auditory belt and parabelt: Hackett and Phillips, 2011; frontal cortex: Berlucchi, 2012) and top-down ipsilateral connections (Winkowski et al., 2018). It is, however, feasible that in our experiments some of the lesioned interhemispheric connections were still or partially intact and subsequently reorganized.

Our finding that the final discrimination performance in control animals and in animals with lesioned projections from the right to the left AC is at the same high level indicates that a commissural information transfer from the right to the left side is not required for solving the task. This corresponds to the dominance of the right AC in processing FM direction and the ability of animals with left-side (but not right-side) AC lesions to finally discriminate FM directions (Wetzel et al., 1998, 2008; Rybalko et al., 2006). We also show that animals with disrupted interhemispheric projections from the left to the right AC have a lower final discrimination performance and H rate than control animals and animals with right-to-left lesions. This suggests that the left AC is nonetheless, albeit not essentially, involved in FM direction discrimination learning. Correspondingly, noninvasive imaging studies in humans have also shown additional left AC activations during FM tone discrimination (Poeppel et al., 2004; Brechmann and Scheich, 2005; König et al., 2008).

We conclude that FM direction discrimination is generally processed by the right AC using mainly inherent spectrotemporal information derived from the ascending auditory pathway and diverse cortical top-down connections but it also uses information from the left AC. The interhemispheric information transfer is mainly required for the rapid acquisition of the task; however, its disruption can be compensated by other, so far unknown mechanisms within a few days. Nevertheless, disturbed left-to-right AC projections generally lead to a destabilized neuronal FM direction processing in the right AC, which limits the individual's H rate and final performance.

Disruption of interhemispheric cross talk does not affect the retrieval of learned FM direction discrimination

While FM direction discrimination learning was impaired, the discrimination performance of animals that learned the task before lesioning interhemispheric neurons was not affected. As shown in the current as well as in several human studies, interhemispheric communication facilitates effective learning of verbal and visual memory (Erickson et al., 2014; Paul et al., 2016) and other complex, attention demanding tasks (Banich, 1998; Weissman and Banich, 2000; Passarotti et al., 2002; Scalf et al., 2009; Stracke et al., 2009). However, the retrieval of a prior learned task may require other cognitive resources and most likely involves other mechanisms than to establish the association between CS and US. It is well known that specific neuronal networks that represent the behavioral meaning, for example, the category of sounds (Scheich et al., 1997; Selezneva et al., 2006; Weinberger, 2007; Tsunada et al., 2012; Tsunada and Cohen, 2014) are formed during the acquisition of an auditory task within the AC (Ohl et al., 2001; Fritz et al., 2005; Ohl and Scheich, 2005; Scheich et al., 2007; Bagur et al., 2018; Francis et al., 2018) and other brain regions (e.g., PFC: Knight et al., 1999; Stark et al., 2007, 2008; Lee et al., 2009; Marton et al., 2018; OFC: Winkowski et al., 2013). These persistent traces or functional connections (Weinberger, 2004; Fritz et al., 2010; Leske et al., 2015) established before photolytic apoptosis of interhemispheric connections in our animals, are most likely operative despite post-training lesions. Thus, it can be concluded that interhemispheric cross talk serves very specific learning functions; here, in particular during the acquisition of FM direction discrimination.

Disruption of interhemispheric cross talk is not required for gap detection and discrimination

Previous studies in gerbils and rats using unilateral and bilateral AC lesioned animals revealed that the gap detection (i.e., discrimination between continuous and segmented FMs) is not affected by unilateral but bilateral AC ablations (Syka et al., 2002; Wetzel et al., 2008; Rybalko et al., 2010). Our data contribute to these results and expand them by demonstrating that auditory interhemispheric cross talk is also not required to solve this task. It was furthermore demonstrated that the discrimination of gap durations (10–30 ms) in segmented FMs is impaired by left (but not right) AC lesions (Wetzel et al., 2008). In contrast to our expectations derived from this data, our current results did not show lesion effects of interhemispheric cross talk on gap discrimination. In contrast to earlier work (Wetzel et al., 2008), we also did not observe a linear or monotonic relationship between gap length and response rate in control animals for the same stimulus set. Instead, a linear relationship was found for shorter gap durations, implying that the FM gap detection threshold of gerbils tested in a negative-reinforcement paradigm is around 10 ms. This is in general agreement with other findings on gerbils (Gleich et al., 2006 and references therein) as well as on other species (e.g., monkey: Petkov et al., 2003 and references therein); however, among additional factors (e.g., sound pressure level, age, behavioral paradigm) the stimulus type, in which the gaps have to be detected, plays an important role as well. For example, when gaps are embedded in white or broad band noise, thresholds are lower (gerbil, <4 ms: Wagner et al., 2003; Hamann et al., 2004; rat, 2 ms: Rybalko et al., 2010; human, 2–3 ms: Phillips et al., 1998). Nevertheless, although research on stimulus generalization indicates that the particular training procedures influence the form of gradients obtained (Honig and Urcuioli, 1981),

there is no evidence that animals exposed to the short versus long stimulus set developed different strategies allowing for a common analysis. We found that across stimulus sets lesioned and control animals responded in a similar way to segmented FM with varying gap durations. Further, all groups displayed stimulus generalization such that stimuli with perceived gaps were classified as CS-. Our results thus indicate that lesioned animals have no different perception or strategies than control animals to cope with ambiguous stimuli.

In conclusion, by using similar stimuli and training paradigms, which have been demonstrated to encompass lateralized auditory processing in various species, we could show by a selective disruption of the interhemispheric connections between the left and right AC that interhemispheric cross talk plays an important role during the acquisition learning of FM direction discrimination. Although the final performance of some lesioned animals does not reach the level of healthy controls, the disturbed learning process may be compensated by other, so far unknown mechanisms. The retrieval of already learned FM direction discrimination does not critically depend on interhemispheric cross talk since it may already be manifested in specialized circuitries of the dominant right hemisphere. There are, however, lateralized auditory brain functions such as gap detection and discrimination, which do not seem to require interhemispheric interactions for learning.

Our study may contribute to a better understanding of mechanisms underlying potential interhemispheric cross talk-dependent pathologies such as auditory verbal hallucinations in schizophrenia (Mulert et al., 2011; Steinmann et al., 2014, 2019), tinnitus (Chen et al., 2015), developmental language impairment (Northam et al., 2012), as well as dyslexia (Henderson et al., 2007), and may provide a useful methodological approach for their experimental investigation.

References

- Albouy P, Benjamin L, Morillon B, Zatorre RJ (2020) Distinct sensitivity to spectrotemporal modulation supports brain asymmetry for speech and melody. *Science* 367:1043–1047.
- Bagur S, Averseng M, Elgueda D, David S, Fritz J, Yin P, Shamma S, Boubenec Y, Ostojic S (2018) Go/No-Go task engagement enhances population representation of target stimuli in primary auditory cortex. *Nat Commun* 9:2529.
- Bajo VM, Nodal FR, Moore DR, King AJ (2010) The descending corticocollicular pathway mediates learning-induced auditory plasticity. *Nat Neurosci* 13:253–260.
- Bamiou DE, Sisodiya S, Musiek FE, Luxon LM (2007) The role of the interhemispheric pathway in hearing. *Brain Res Rev* 56:170–182.
- Banich MT (1998) The missing link: the role of interhemispheric interaction in attentional processing. *Brain Cogn* 36:128–157.
- Bartolomeo P, Thiebaut de Schotten M (2016) Let thy left brain know what thy right brain doeth: inter-hemispheric compensation of functional deficits after brain damage. *Neuropsychologia* 93:407–412.
- Berlucchi G (2012) Frontal callosal disconnection syndromes. *Cortex* 48:36–45.
- Bitan T, Lifshitz A, Breznitz Z, Booth JR (2010) Bidirectional connectivity between hemispheres occurs at multiple levels in language processing but depends on sex. *J Neurosci* 30:11576–11585.
- Blackmon K, Pardoe HR, Barr WB, Ardekani BA, Doyle WK, Devinsky O, Kuzniecky R, Thesen T (2015) The corpus callosum and recovery of working memory after epilepsy surgery. *Epilepsia* 56:527–534.
- Bloom JS, Hynd GW (2005) The role of the corpus callosum in interhemispheric transfer of information: excitation or inhibition? *Neuropsychol Rev* 15:59–71.
- Boemio A, Fromm S, Braun A, Poeppel D (2005) Hierarchical and asymmetric temporal sensitivity in human auditory cortices. *Nat Neurosci* 8:389–395.

- Brechmann A, Scheich H (2005) Hemispheric shifts of sound representation in auditory cortex with conceptual listening. *Cereb Cortex* 15:578–587.
- Budinger E (2020) Primary auditory cortex and the thalamo-cortico-thalamic circuitry I. Anatomy. In: *The senses: a comprehensive reference*, Ed 2 (Fritzsch B, ed), pp 623–656. Oxford: Elsevier.
- Budinger E, Heil P, Scheich H (2000) Functional organization of auditory cortex in the Mongolian gerbil (*Meriones unguiculatus*). III. Anatomical subdivisions and corticocortical connections. *Eur J Neurosci* 12:2425–2451.
- Carrasco A, Brown TA, Kok MA, Chabot N, Kral A, Lomber SG (2013) Influence of core auditory cortical areas on acoustically evoked activity in contralateral primary auditory cortex. *J Neurosci* 33:776–789.
- Chen YC, Xia W, Feng Y, Li X, Zhang J, Feng X, Wang CX, Cai Y, Wang J, Salvi R, Teng GJ (2015) Altered interhemispheric functional coordination in chronic tinnitus patients. *Biomed Res Int* 2015:345647.
- Cipolloni PB, Peters A (1983) The termination of callosal fibres in the auditory cortex of the rat. A combined Golgi–electron microscope and degeneration study. *J Neurocytol* 12:713–726.
- Clarke JM, Zaidel E (1994) Anatomical-behavioral relationships: corpus callosum morphometry and hemispheric specialization. *Behav Brain Res* 64:185–202.
- Code RA, Winer JA (1985) Commissural neurons in layer III of cat primary auditory cortex (AI): pyramidal and non-pyramidal cell input. *J Comp Neurol* 242:485–510.
- Concha ML, Bianco IH, Wilson SW (2012) Encoding asymmetry within neural circuits. *Nat Rev Neurosci* 13:832–843.
- Conti F, Manzoni T (1994) The neurotransmitters and postsynaptic actions of callosally projecting neurons. *Behav Brain Res* 64:37–53.
- Corballis MC, Häberling IS (2017) The many sides of hemispheric asymmetry: a selective review and outlook. *J Int Neuropsychol Soc* 23:710–718.
- de Haan EHF, Corballis PM, Hillyard SA, Marzi CA, Seth A, Lamme VAF, Volz L, Fabri M, Schechter E, Bayne T, Corballis M, Pinto Y (2020) Split-brain: what we know now and why this is important for understanding consciousness. *Neuropsychol Rev* 30:224–233.
- Erickson RL, Paul LK, Brown WS (2014) Verbal learning and memory in agenesis of the corpus callosum. *Neuropsychologia* 60:121–130.
- Francis NA, Elgueda D, Englitz B, Fritz JB, Shamma SA (2018) Laminar profile of task-related plasticity in ferret primary auditory cortex. *Sci Rep* 8:16375.
- Fritz J, Elhilali M, Shamma S (2005) Active listening: task-dependent plasticity of spectrotemporal receptive fields in primary auditory cortex. *Hear Res* 206:159–176.
- Fritz JB, David SV, Radtke-Schuller S, Yin P, Shamma SA (2010) Adaptive, behaviorally gated, persistent encoding of task-relevant auditory information in ferret frontal cortex. *Nat Neurosci* 13:1011–1019.
- Gazzaniga MS (2005) Forty-five years of split-brain research and still going strong. *Nat Rev Neurosci* 6:653–659.
- Gleich O, Hamann I, Kittel MC, Klump GM, Strutz J (2006) A quantitative analysis of psychometric functions for different auditory tasks in gerbils. *Hear Res* 220:27–37.
- Güntürkün O, Ströckens F, Ocklenburg S (2020) Brain lateralization: a comparative perspective. *Physiol Rev* 100:1019–1063.
- Hackett TA, Phillips DP (2011) The commissural auditory system. In: *The auditory cortex* (Winer JA and Schreiner CE, eds), pp 197–222. New York: Springer.
- Hamann I, Gleich O, Klump GM, Kittel MC, Strutz J (2004) Age-dependent changes of gap detection in the Mongolian gerbil (*Meriones unguiculatus*). *J Assoc Res Otolaryngol* 5:49–57.
- Harris LJ (2019) The discovery of cerebral specialization. *Front Neurol Neurosci* 44:1–14.
- Henderson L, Barca L, Ellis AW (2007) Interhemispheric cooperation and non-cooperation during word recognition: evidence for callosal transfer dysfunction in dyslexic adults. *Brain Lang* 103:276–291.
- Hervé PY, Zago L, Petit L, Mazoyer B, Tzourio-Mazoyer N (2013) Revisiting human hemispheric specialization with neuroimaging. *Trends Cogn Sci* 17:69–80.
- Homma NY, Happel MFK, Nodal FR, Ohl FW, King AJ, Bajo VM (2017) A role for auditory corticothalamic feedback in the perception of complex sounds. *J Neurosci* 37:6149–6161.
- Honig WK, Urciuoli PJ (1981) The legacy of Guttman and Kalish (1956): twenty-five years of research on stimulus generalization. *J Exp Anal Behav* 36:405–445.
- Hutsler J, Galuske RAW (2003) Hemispheric asymmetries in cerebral cortical networks. *Trends Neurosci* 26:429–435.
- Josse G, Tzourio-Mazoyer N (2004) Hemispheric specialization for language. *Brain Res Brain Res Rev* 44:1–12.
- Karayannis T, Huerta-Ocampo I, Capogna M (2007) GABAergic and pyramidal neurons of deep cortical layers directly receive and differently integrate callosal input. *Cereb Cortex* 17:1213–1226.
- Kitzes LM, Doherty D (1994) Influence of callosal activity on units in the auditory cortex of ferret (*Mustela putorius*). *J Neurophysiol* 71:1740–1751.
- Knight RT, Staines WR, Swick D, Chao LL (1999) Prefrontal cortex regulates inhibition and excitation in distributed neural networks. *Acta Psychol (Amst)* 101:159–178.
- König R, Sieluzycy C, Simserides C, Heil P, Scheich H (2008) Effects of the task of categorizing FM direction on auditory evoked magnetic fields in the human auditory cortex. *Brain Res* 1220:102–117.
- Lee CC, Winer JA (2008) Connections of cat auditory cortex: II. Commissural system. *J Comp Neurol* 507:1901–1919.
- Lee JH, Russ BE, Orr LE, Cohen YE (2009) Prefrontal activity predicts monkeys' decisions during an auditory category task. *Front Integr Neurosci* 3:16.
- Leske S, Ruhnau P, Frey J, Lithari C, Müller N, Hartmann T, Weisz N (2015) Prestimulus network integration of auditory cortex predisposes near-threshold perception independently of local excitability. *Cereb Cortex* 25:4898–4907.
- Macklis JD (1993) Transplanted neocortical neurons migrate selectively into regions of neuronal degeneration produced by chromophore-targeted laser photolysis. *J Neurosci* 13:3848–3863.
- Madison RD, Macklis JD (1993) Noninvasively induced degeneration of neocortical pyramidal neurons in vivo: selective targeting by laser activation of retrogradely transported photolytic chromophore. *Exp Neurol* 121:153–159.
- Magavi SS, Leavitt BR, Macklis JD (2000) Induction of neurogenesis in the neocortex of adult mice. *Nature* 405:951–955.
- Marton TF, Seifkar H, Luongo FJ, Lee AT, Sohal VS (2018) Roles of prefrontal cortex and mediodorsal thalamus in task engagement and behavioral flexibility. *J Neurosci* 38:2569–2578.
- Mulert C, Kirsch V, Pascual-Marqui R, McCarley RW, Spencer KM (2011) Long-range synchrony of γ oscillations and auditory hallucination symptoms in schizophrenia. *Int J Psychophysiol* 79:55–63.
- Northam GB, Liégeois F, Tournier JD, Croft LJ, Johns PN, Chong WK, Wyatt JS, Baldeweg T (2012) Interhemispheric temporal lobe connectivity predicts language impairment in adolescents born preterm. *Brain* 135:3781–3798.
- Ohl FW, Scheich H (2005) Learning-induced plasticity in animal and human auditory cortex. *Curr Opin Neurobiol* 15:470–477.
- Ohl FW, Wetzel W, Wagner T, Rech A, Scheich H (1999) Bilateral ablation of auditory cortex in Mongolian gerbil affects discrimination of frequency modulated tones but not of pure tones. *Learn Mem* 6:347–362.
- Ohl FW, Scheich H, Freeman WJ (2001) Change in pattern of ongoing cortical activity with auditory category learning. *Nature* 412:733–736.
- Païement P, Champoux F, Bacon BA, Lassonde M, Mensour B, Leroux JM, Lepore F (2010) Functional reorganization of the auditory pathways (or lack thereof) in callosal agenesis is predicted by monaural sound localization performance. *Neuropsychologia* 48:601–606.
- Passarotti AM, Banich MT, Sood RK, Wang JM (2002) A generalized role of interhemispheric interaction under attentionally demanding conditions: evidence from the auditory and tactile modality. *Neuropsychologia* 40:1082–1096.
- Paul LK, Erickson RL, Hartman JA, Brown WS (2016) Learning and memory in individuals with agenesis of the corpus callosum. *Neuropsychologia* 86:183–192.
- Petkov CI, O'Connor KN, Sutter ML (2003) Illusory sound perception in macaque monkeys. *J Neurosci* 23:9155–9161.
- Phillips DP, Hall SE, Harrington IA, Taylor TL (1998) “Central” auditory gap detection: a spatial case. *J Acoust Soc Am* 103:2064–2068.
- Poeppel D, Assaneo MF (2020) Speech rhythms and their neural foundations. *Nat Rev Neurosci* 21:322–334.
- Poeppel D, Guillemin A, Thompson J, Fritz J, Bavelier D, Braun AR (2004) Auditory lexical decision, categorical perception, and FM direction discrimination differentially engage left and right auditory cortex. *Neuropsychologia* 42:183–200.

- Pollak GD, Burger RM, Klug A (2003) Dissecting the circuitry of the auditory system. *Trends Neurosci* 26:33–39.
- Radtke-Schuller S, Schuller G, Angenstein F, Grosser OS, Goldschmidt J, Budinger E (2016) Brain atlas of the Mongolian gerbil (*Meriones unguiculatus*) in CT/MRI-aided stereotaxic coordinates. *Brain Struct Funct* 221 Suppl 1:1–272.
- Richter K, Hess A, Scheich H (1999) Functional mapping of transsynaptic effects of local manipulation of inhibition in gerbil auditory cortex. *Brain Res* 831:184–199.
- Rock C, Apicella AJ (2015) Callosal projections drive neuronal-specific responses in the mouse auditory cortex. *J Neurosci* 35:6703–6713.
- Rock C, Zurita H, Lebbly S, Wilson CJ, Apicella AJ (2018) Cortical circuits of callosal GABAergic neurons. *Cereb Cortex* 28:1154–1167.
- Roland JL, Snyder AZ, Hacker CD, Mitra A, Shimony JS, Limbrick DD, Raichle ME, Smyth MD, Leuthardt EC (2017) On the role of the corpus callosum in interhemispheric functional connectivity in humans. *Proc Natl Acad Sci USA* 114:13278–13283.
- Rybalko N, Suta D, Nwabeze-Ogbo F, Syka J (2006) Effect of auditory cortex lesions on the discrimination of frequency-modulated tones in rats. *Eur J Neurosci* 23:1614–1622.
- Rybalko N, Suta D, Popelár J, Syka J (2010) Inactivation of the left auditory cortex impairs temporal discrimination in the rat. *Behav Brain Res* 209:123–130.
- Saldeitis K, Happel MFK, Ohl FW, Scheich H, Budinger E (2014) Anatomy of the auditory thalamocortical system in the Mongolian gerbil: nuclear origins and cortical field-, layer-, and frequency-specificities. *J Comp Neurol* 522:2397–2430.
- Saldeitis K, Jeschke M, Budinger E, Ohl FW, Happel MFK (2021) Laser-induced apoptosis of corticothalamic neurons in layer VI of auditory cortex impact on cortical frequency processing. *Front Neural Circuits* 15:659280.
- Scaif PE, Banich MT, Erickson AB (2009) Interhemispheric interaction expands attentional capacity in an auditory selective attention task. *Exp Brain Res* 194:317–322.
- Scheich H, Stark H, Zuschratter W, Ohl FW, Simonis CE (1997) Some functions of primary auditory cortex in learning and memory formation. *Adv Neurol* 73:179–193.
- Scheich H, Brechmann A, Brosch M, Budinger E, Ohl FW (2007) The cognitive auditory cortex: task-specificity of stimulus representations. *Hear Res* 229:213–224.
- Schönwiesner M, Rübsamen R, von Cramon DY (2005) Spectral and temporal processing in the human auditory cortex—revisited. *Ann NY Acad Sci* 1060:89–92.
- Schulze H, Deutscher A, Tziridis K, Scheich H (2014) Unilateral auditory cortex lesions impair or improve discrimination learning of amplitude modulated sounds, depending on lesion side. *PLoS One* 9:e87159.
- Scott SK, McGettigan C (2013) Do temporal processes underlie left hemisphere dominance in speech perception? *Brain Lang* 127:36–45.
- Selezneva E, Scheich H, Brosch M (2006) Dual time scales for categorical decision making in auditory cortex. *Curr Biol* 16:2428–2433.
- Slater BJ, Isaacson JS (2020) Interhemispheric callosal projections sharpen frequency tuning and enforce response fidelity in primary auditory cortex. *eNeuro* 7:ENEURO.0256-20.2020.
- Stark H, Rothe T, Deliano M, Scheich H (2007) Theta activity attenuation correlates with avoidance learning progress in gerbils. *Neuroreport* 18:549–552.
- Stark H, Rothe T, Deliano M, Scheich H (2008) Dynamics of cortical theta activity correlates with stages of auditory avoidance strategy formation in a shuttle-box. *Neuroscience* 151:467–475.
- Steinmann S, Leicht G, Mulert C (2014) Interhemispheric auditory connectivity: structure and function related to auditory verbal hallucinations. *Front Hum Neurosci* 8:55.
- Steinmann S, Leicht G, Mulert C (2019) The interhemispheric miscommunication theory of auditory verbal hallucinations in schizophrenia. *Int J Psychophysiol* 145:83–90.
- Stracke H, Okamoto H, Pantev C (2009) Interhemispheric support during demanding auditory signal-in-noise processing. *Cereb Cortex* 19:1440–1447.
- Sun T, Walsh CA (2006) Molecular approaches to brain asymmetry and handedness. *Nat Rev Neurosci* 7:655–662.
- Syka J, Rybalko N, Mazelová J, Druga R (2002) Gap detection threshold in the rat before and after auditory cortex ablation. *Hear Res* 172:151–159.
- Tervaniemi M, Hugdahl K (2003) Lateralization of auditory-cortex functions. *Brain Res Brain Res Rev* 43:231–246.
- Thomas H, López V (2003) Comparative study of inter- and intrahemispheric cortico-cortical connections in gerbil auditory cortex. *Biol Res* 36:155–169.
- Toga AW, Thompson PM (2003) Mapping brain asymmetry. *Nat Rev Neurosci* 4:37–48.
- Tsunada J, Cohen YE (2014) Neural mechanisms of auditory categorization: from across brain areas to within local microcircuits. *Front Neurosci* 8:161.
- Tsunada J, Lee JH, Cohen YE (2012) Differential representation of auditory categories between cell classes in primate auditory cortex. *J Physiol* 590:3129–3139.
- van der Knaap LJ, van der Ham IJ (2011) How does the corpus callosum mediate interhemispheric transfer? A review. *Behav Brain Res* 223:211–221.
- Wagner E, Klump GM, Hamann I (2003) Gap detection in Mongolian gerbils (*Meriones unguiculatus*). *Hear Res* 176:11–16.
- Weinberger NM (2004) Specific long-term memory traces in primary auditory cortex. *Nat Rev Neurosci* 5:279–290.
- Weinberger NM (2007) Auditory associative memory and representational plasticity in the primary auditory cortex. *Hear Res* 229:54–68.
- Weissman DH, Banich MT (2000) The cerebral hemispheres cooperate to perform complex but not simple tasks. *Neuropsychology* 14:41–59.
- Westerhausen R, Grüner R, Specht K, Hugdahl K (2009) Functional relevance of interindividual differences in temporal lobe callosal pathways: a DTI tractography study. *Cereb Cortex* 19:1322–1329.
- Wetzel W, Ohl FW, Wagner T, Scheich H (1998) Right auditory cortex lesion in Mongolian gerbils impairs discrimination of rising and falling frequency-modulated tones. *Neurosci Lett* 252:115–118.
- Wetzel W, Ohl FW, Scheich H (2008) Global versus local processing of frequency-modulated tones in gerbils: an animal model of lateralized auditory cortex functions. *Proc Natl Acad Sci USA* 105:6753–6758.
- Winkowski DE, Bandyopadhyay S, Shamma SA, Kanold PO (2013) Frontal cortex activation causes rapid plasticity of auditory cortical processing. *J Neurosci* 33:18134–18148.
- Winkowski DE, Nagode DA, Donaldson KJ, Yin P, Shamma SA, Fritz JB, Kanold PO (2018) Orbitofrontal cortex neurons respond to sound and activate primary auditory cortex neurons. *Cereb Cortex* 28:868–879.
- Zatorre RJ, Belin P, Penhune VB (2002) Structure and function of auditory cortex: music and speech. *Trends Cogn Sci* 6:37–46.